Advanced High-Order Algorithms for High-Fidelity Simulation of Unsteady Flows over Complex Geometries

Grant Number: FA9550-10-1-0418

PI: Antony Jameson

Aeronautics and Astronautics Department
Stanford University, CA, US

AFOSR Program Review
June 01, 2011

Acknowledgement

The current research is made possible by the support of

- the Airforce Office of Scientific Research under grant FA9550-10-1-0418 by Dr. Fariba Fahroo
- the National Science Foundation under grants 0708071 and 0915006 monitored by Dr. Leland Jameson

Research Personnel in the Stanford Aerospace Computing Laboratory

- Postdoc : Peter Vincent (now to be a Lecturer at Imperial College)
- Doctoral Students:
  - Patrice Castonguay
  - Kui Ou
  - Lala Li
  - Yves Allenau
  - David Williams
  - Matt Culbreth

Overview

During the last year ACL research on high-order methods has been simultaneously directed at

- Theory:
  - Formulation of energy stable schemes for arbitrary order of accuracy for general elements
- Implementation:
  - Development of new software SD++ for 2D and 3D problems on mixed meshes written in C++ and also in Cuda for GPUs.
- Applications:
  - Flows with moving boundaries
  - Transitional flows
  - Flow past spinning sphere
  - Flow past flapping wings

Overview of High-order Schemes for Linear Advection

Nodal Discontinuous Galerkin Scheme for Linear Advection

introducing collocation points x_j in each element and define the local solution by the Lagrange polynomial of degree $p = n - 1$.

$$u_h^k = \sum_{j=1}^{n} u_j l_j(x)$$

where u_h^k is the discrete solution in element k in the interval [-1,1]. The discrete residual in the element k is written as

$$R_h^k = \frac{\partial u_h^k}{\partial t} + \frac{\partial f(u_h^k)}{\partial x}$$

The Galerkin method requires the residual of the equation to be orthogonal to the basis functions. Apply IBP twice, the nodal DG scheme in strong form is:

$$\int_{-1}^{1} \frac{\partial u_h^k}{\partial t} l_j dx + \int_{-1}^{1} l_j \frac{\partial f(u_h^k)}{\partial x} dx + [\hat{f} - f(u_h^k)] l_j \Big|_{-1}^{1} = 0$$

where $\hat{f}$ is the numerical flux at the element interface.

Nodal Discontinuous Galerkin Scheme for Linear Advection

Alternatively expressed the NDG scheme in matrix form as:

$$\mathbf{M^k}\frac{d\mathbf{u}}{dt}+\mathbf{S^k f}+\mathbf{l}(\hat{f}-f)\Big|_{x_L}^{x_R}=0 \text{ where } \mathbf{M^k}_{ij}=\int_{-1}^{1}\frac{(x_R-x_L)}{2}l_i l_j dx \text{ and } \mathbf{S^k}_{ij}=\int_{-1}^{1} l_i l_j' dx$$

Follow the flux reconstruction pocedure proposed by Huynh and rewrite the flux at each boundary as

$$\hat{f}(-1)=au_h(-1)+f_{CL}, \quad \hat{f}(1)=au_h(1)+f_{CR}$$

where f_{CL} and f_{CR} are boundary corrections

$$f_{CL}=\hat{f}(-1)-au_h(-1), \quad f_{CR}=\hat{f}(1)-au_h(1)$$

With these, and for simplicity assuming upwind flux so there is no correction on the right, the strong form of the nodal DG scheme can alternatively be expressed as

$$\mathbf{M^k}\frac{d\mathbf{u}}{dt}+\mathbf{S^k f}-f_{CL}\mathbf{l}(x_L)=0$$

Spectral Difference Scheme for Linear Advection

the discrete solution is locally represented by Lagrange polynomial on the solution collocation points x_j as

$$u_h = \sum_{j=1}^{n} u_j l_j(x) \text{ ,with } u_h \text{ spans [-1,1]}$$

where for polynomials of degree p, $n = p+1$.Represent the flux by a separate Lagrange polynomial, $\hat{l}_j(x)$, of degree $p+1$, defined by the $n+1$ flux collocation points $\hat{x}_j$

$$f_h = \sum_{j=1}^{n+1} f_j \hat{l}_j(x)$$

The interior values at the flux collocation points $f_j = f(u_h(\hat{x}_j))$ where $u_h(\hat{x}_j)$ is interpolated from $u_h(x)$. The discrete flux can be expanded and rewritten as

$$f_h(x) = f_{CL}\hat{l}_1(x) + \sum_{j=1}^{n+1} f_j \hat{l}_j(x) + f_{CR}\hat{l}_{n+1}(x) = f_{CL}\hat{l}_1(x) + a u_h(x) + f_{CR}\hat{l}_{n+1}(x)$$

Spectral Difference Scheme for Linear Advection

Differentiating the flux polynomial at the solution collocation to obtain the SD scheme

$$\frac{\partial u_h}{\partial t} + \left[a\frac{\partial u_h(x)}{\partial x} + f_{CL}\hat{l}_1'(x) + f_{CR}\hat{l}_{n+1}'(x) \right] = 0$$

Cast the SD scheme in matrix form

$$\frac{du_i}{dt} + \left[a\sum_{j=1}^{n} \mathbf{D}_{ij}u_j + f_{CL}\frac{d\hat{l}_1}{dx}(x_i) + f_{CR}\frac{d\hat{l}_{n+1}}{dx}(x_i) \right] = 0, \quad \textit{where} \;\; \mathbf{D} = \mathbf{M}^{-1}\mathbf{S}$$

Multiply the equation by the mass matrix, and assuming upwind flux like before to get

$$\sum_j \mathbf{M_{ij}}\frac{du_i}{dt} + a\sum_{j=1}^{n} \mathbf{S}_{ij}u_j + f_{CL}\sum_j \mathbf{M_{ij}}\hat{l}_1'(x_i) = 0$$

Expanding the mass matrix in the last term, this can be further reduced to

$$\sum_j \mathbf{M_{ij}}\frac{du_i}{dt} + a\sum_{j=1}^{n} \mathbf{S}_{ij}u_j - f_{CL}l_i(-1) = f_{CL}\int_{-1}^{1} l_i'(x)\hat{l}_1(x)dx$$

Flux Reconstruction Scheme for Linear Advection

the discrete solution is locally represented by Lagrange polynomial on the solution collocation points x_j as

$$u_h = \sum_{j=1}^{n} u_j l_j(x)$$

In the FR scheme, the continous $f_j(x)$ is now made up of an interior flux term f_j^D and a correction flux term f_j^C.

$$f_h^D = \sum_{j=1}^{n+1} f_j^D l_j(x)$$

The interfaces $f_h^D(-1)$ and $f_h^D(1)$ are the interpolated values from $f_h^D(x)$. The deviation from the desired continuous flux f_j is

$$f_h^C(-1) = f_{CL} = f_h(-1) - f_h^D(-1) = \hat{f}(-1) - f_h^D(-1)$$

Consider a degree $k+1$ correction function $g_L = g_L(r)$ and $g_R = g_R(r)$ that approximate zero (in some sense) within the element while satisfying

$$g_L(-1) = 1, \;\; g_L(1) = 0 \;\; \& \;\; g_R(-1) = 0, \;\; g_R(1) = 1$$

Flux Reconstruction Scheme for Linear Advection

A suitable expression for f^C can now be written in terms of g_L and g_R as

$$f_h^C = f_{CL}\, g_L + f_{CR}\, g_R$$

The discrete flux f_h that has continuous values across the element can now be constructed as follows

$$f_h = f_h^D + f_h^C$$

Finally we differentiate the flux at the solution collocation points to obtain

$$\frac{du_i}{dt} + \left[\sum_{j=1}^{n+1} f_j^D \frac{dl_j}{dx}(x_i) + f_{CL}\frac{dg_L}{dx}(x_i) + f_{CR}\frac{dg_R}{dx}(x_i)\right] = 0$$

or for linear advection with $f = au$, this can be written as

$$\frac{du_i}{dt} + \left[a\sum_{j=1}^{n+1} u_j \frac{dl_j}{dx}(x_i) + f_{CL}\frac{dg_L}{dx}(x_i) + f_{CR}\frac{dg_R}{dx}(x_i)\right] = 0$$

This form of Flux Reconstruction scheme resembles the form of the SD scheme.

Summary: NDG vs SD

NDG

$$\mathbf{M^k}\frac{d\mathbf{u}}{dt} + a\mathbf{S^k u} - f_{CL} l(x_L) = 0$$

SD

$$\mathbf{M}\frac{d\mathbf{u}}{dt} + a\mathbf{Su} - f_{CL} l(-1) = f_{CL} \int_{-1}^{1} l_i'(x)\hat{l}_1(x)dx$$

Summary: SD vs FR

SD

$$\frac{\partial u_h}{\partial t} + \left[a \frac{\partial u_h(x)}{\partial x} + f_{CL} \hat{l}'_1(x) + f_{CR} \hat{l}'_{n+1}(x) \right] = 0$$

FR

$$\frac{du_i}{dt} + \left[a \sum_{j=1}^{n+1} u_j \frac{dl_j}{dx}(x_i) + f_{CL} \frac{dg_L}{dx}(x_i) + f_{CR} \frac{dg_R}{dx}(x_i) \right] = 0$$

Overview of Energy Stability

Energy Estimate for Linear Advection

Linear advection equation:

$$\frac{\partial u}{\partial t} + a\frac{\partial u}{\partial x} = 0$$

Consider the energy estimate for the linear advection by multiplying the linear advection equation by u and integrate over the domain x that spans [a,b],

$$\int_a^b u\left(\frac{\partial u}{\partial t} + a\frac{\partial u}{\partial x}\right)dx = 0$$

which, after expansion, shows it satisfies the energy estimate,

$$\frac{d}{dt}\int_a^b \frac{u^2}{2}dx = \frac{1}{2}a(u_a^2 - u_b^2)$$

Energy Stability Proof for Nodal Discontinuous Galerkin

In Hesthaven [**?**], the stability of the nodal discontinuous Galerkin method has been proved for the linear advection equation. Taking the strong form of the discretized linear advection equation, and multiply it with the local solution to obtain

$$\mathbf{u}^T \mathbf{M}^k \frac{d\mathbf{u}}{dt} + \mathbf{u}^T \mathbf{S^k f} + \mathbf{u}^T \mathbf{l}(\hat{f} - f)\Big|_{x_L}^{x_R} = 0$$

Since M^k and S^k have been pre-integrated exactly, this is equivalent to

$$\frac{d}{dt}\int_{x_L}^{x_R} \frac{u_h^2}{2} dx + a\int_{x_L}^{x_R} u_h \frac{\partial u_h}{\partial x} dx + u_h(\hat{f} - a u_h)\Big|_{x_L}^{x_R} = 0$$

Here the middle term can be integrated and combined with the last term

$$\frac{d}{dt}\int_{x_L}^{x_R} \frac{u_h^2}{2} dx = -(u_h \hat{f} - a\frac{u_h^2}{2})\Big|_{x_L}^{x_R}$$

It can be shown that there is a negative contribution at every element boundary except the inflow boundary, which is strictly less than the true boundary contribution.

Energy Stability Proof Strategy for Spectral Difference

$$\frac{du_i}{dt} + \left[a \sum_{j=1}^{n} \mathbf{D}_{ij} u_j + f_{CL} \frac{d\hat{l}_1}{dx}(x_i) + f_{CR} \frac{d\hat{l}_{n+1}}{dx}(x_i) \right] = 0, \quad where \;\; \mathbf{D} = \mathbf{M}^{-1}\mathbf{S}$$

$$\sum_j \mathbf{M_{ij}} \frac{du_i}{dt} + a \sum_{j=1}^{n} \mathbf{S}_{ij} u_j + f_{CL} \sum_j \mathbf{M_{ij}} \hat{l}_1'(x_i)$$

$$= \sum_j \mathbf{M_{ij}} \frac{du_i}{dt} + a \sum_{j=1}^{n} \mathbf{S}_{ij} u_j - f_{CL} l_i(-1) - f_{CL} \int_{-1}^{1} l_i'(x) \hat{l}_1(x) dx$$

A new matrix **Q** is proposed in place of the mass matrix **M** so that its introduction leads the SD scheme to the following form,

$$\sum_j \mathbf{Q_{ij}} \frac{du_i}{dt} + a \sum_{j=1}^{n} \mathbf{S}_{ij} u_j + f_{CL} \sum_j \mathbf{Q_{ij}} \hat{l}_1'(x_i) = \sum_j \mathbf{Q_{ij}} \frac{du_i}{dt} + a \sum_{j=1}^{n} \mathbf{S}_{ij} u_j - f_{CL} l_i(-1) = 0$$

If a suitable **Q** can be identified as above so that the basic form is retained while the term that differentiates DG and SD is removed or absorbed, we can attain an energy estimate for the SD scheme with the norm $\mathbf{u^T Q u}$ replacing the norm $\mathbf{u^T M u}$ in the nodal DG scheme in each element.

Energy Stability Proof for Spectral Difference

The requirements for **Q** can be summarized as follows,

1. It has the following form $\mathbf{Q} = \mathbf{M} + \mathbf{C}$
2. It retains the function of the mass matrix and satisfies $\mathbf{QD} = \mathbf{S}$
3. The last two requirements lead to the third requirement that $\mathbf{CD} = \mathbf{0}$
4. The expansion of the follwing term eliminates the term that differentiates the SD and DG schemes such that $f_{CL} \sum_j \mathbf{Q_{ij}} \hat{l}_1'(x_i) = f_{CL} l_i(-1)$

It is shown by Jameson [?] that the above requirements can indeed be satisfied by choosing the matrix

$$\mathbf{Q} = \mathbf{M} + cdd^T$$

where d^T is the p^{th} difference operator. The first, second and third requirements are satisfied, since for any polynomial $R_p(x)$ of degree p, the combined operation by d and **D** on $R_p(x)$ leads to $(p+1)^{th}$ derivative on p^{th} degree polynomial, which is zero.

$$\sum_j d_i \sum_j D_{ij} R_p(x_j) = R_p^{p+1} = 0$$

This leaves only the parameter c to be determined which can satisfy the last requirement.

Energy Stability Proof for Spectral Difference

It is shown that this is possible by picking c as

$$c = \frac{2p}{2p+1}\frac{1}{c_p^2}\frac{1}{p!(p+1)!} > 0$$

where $c_p = \frac{1 \cdot 3 \cdot 5 \ldots (2p-1)}{p!}$ is the leading coefficients of the Legendre polynomial $L_p(x)$ of degree p. With this choice of $\mathbf{C} = cdd^T$ and $\mathbf{Q} = \mathbf{M} + \mathbf{C}$, the SD scheme becomes,

$$\sum_j \mathbf{Q_{ij}} \frac{du_i}{dt} + a \sum_{j=1}^{n} \mathbf{S}_{ij} u_j - f_{CL} l_i(-1) = 0$$

and now the same argument that was used to prove the energy stability of the nodal DG shceme establishes the energy stability of the SD scheme with the norm

$$||u|| = \int \left(u^2 + c \left(\frac{\partial^p u}{\partial x^p} \right)^2 \right) dx$$

for the case of solution polynomial of degree p, provided the interior flux collocation points are the zeros of the Legendre polynomial $L_p(x)$.

Energy Stability Proof for Flux Reconstruction

From the earlier section, we derived the energy estimate for the SD scheme using boundary flux corrections in a way very similar to the Flux Reconstruction scheme. The connection between the two schemes are (to some degree) implied by the similarity of the final forms of the schemes. Hence it is also plausible to approach the energy estimate of the FR scheme using a similar norm of the form

$$||u|| = \int u^2 + c_0 \left(\frac{\partial^p u}{\partial x^p} \right)^2 dx$$

where c_0 for FR scheme is to be determined.

Energy Stability Proof for Flux Reconstruction

From Vincent, Castonguay and Jameson (2010), the first term can be written as

$$\frac{d}{dt}\int_{-1}^{1} u_j^2 dx = -\hat{a}[u_R^2 - u_L^2] - 2f_{CL}\left(-u_L - \int_{-1}^{1} g_L \frac{\partial u_h}{\partial x} dx\right) - 2f_{CR}\left(u_R - \int_{-1}^{1} g_R \frac{\partial u_h}{\partial x} dx\right)$$

and for the second term, setting $c_0 = \frac{c}{2}$,

$$\frac{1}{2}\frac{d}{dt}\int_{-1}^{1} c\left(\frac{\partial^p u_h}{\partial x^p}\right)^2 dx = -2cf_{CL}\left(\frac{\partial^p u_h}{\partial x^p}\right)\left(\frac{d^{p+1} g_L}{dx^{p+1}}\right) - 2cf_{CR}\left(\frac{\partial^p u_h}{\partial x^p}\right)\left(\frac{d^{p+1} g_R}{dx^{p+1}}\right)$$

adding the two equations together we obtain the desired explicit expression as

$$\begin{aligned}\frac{d}{dt}\int_{-1}^{1} u_j^2 + \frac{c}{2}\left(\frac{\partial^p u_j}{\partial x^p}\right)^2 dx = &+ 2(f_{CL}u_L - \hat{a}\frac{u_L^2}{2}) - 2(f_{CR}u_R - \hat{a}\frac{u_R^2}{2}) \\ &+ 2f_{CL}\left[\int_{-1}^{1} g_L \frac{\partial u_h}{\partial x} dx - c\left(\frac{\partial^p u_h}{\partial x^p}\right)\left(\frac{d^{p+1} g_L}{dx^{p+1}}\right)\right] \\ &+ 2f_{CR}\left[\int_{-1}^{1} g_R \frac{\partial u_h}{\partial x} dx - c\left(\frac{\partial^p u_h}{\partial x^p}\right)\left(\frac{d^{p+1} g_R}{dx^{p+1}}\right)\right]\end{aligned}$$

Difference between NDG and FR

Energy Norm of NDG

$$\frac{d}{dt}\int_{x_L}^{x_R}\frac{u_h^2}{2}dx = -(u_h\hat{f} - a\frac{u_h^2}{2})\Big|_{x_L}^{x_R}$$

Energy Norm of FR

$$\frac{d}{dt}\int_{-1}^{1} u_j^2 + \frac{c}{2}\left(\frac{\partial^p u_j}{\partial x^p}\right)^2 dx = +2(f_{CL}u_L - \hat{a}\frac{u_L^2}{2}) - 2(f_{CR}u_R - \hat{a}\frac{u_R^2}{2})$$

Energy Stability Proof for Flux Reconstruction

Vincent, Castonguay and Jameson have shown that the FR scheme is energy stable if

1. Condition a: $\int_{-1}^{1} g_L \frac{\partial u_h}{\partial x} dx - c\left(\frac{\partial^p u_h}{\partial x^p}\right)\left(\frac{d^{p+1}g_L}{dx^{p+1}}\right) = 0$
2. Condition b: $\int_{-1}^{1} g_R \frac{\partial u_h}{\partial x} dx - c\left(\frac{\partial^p u_h}{\partial x^p}\right)\left(\frac{d^{p+1}g_R}{dx^{p+1}}\right) = 0$
3. Condition c: $c_0(k) < c < \infty$, where $c_0(k) = \frac{-2}{(2k+1)(a_k k!)^2}$

Energy Stable Correction Functions

These three equations can be solved and the final expressions for the left and right flux correction functions in terms of Legendre polynomials are written as

$$g_L = \frac{(-1)^k}{2}\left[L_k - \left(\frac{\eta_k L_{k-1} + L_{k+1}}{1+\eta_k}\right)\right]$$

$$g_R = \frac{(+1)^k}{2}\left[L_k + \left(\frac{\eta_k L_{k-1} + L_{k+1}}{1+\eta_k}\right)\right]$$

where $\eta_k = \frac{c(2k+1)(a_k k!)^2}{2}$. Use of these correction functions leads to energy stable FR schemes with a suitable c.

Examples of ESFR Scheme - Nodal DG

$$g_L = \frac{(-1)^k}{2}(L_k - L_{k+1}) \ , \ g_R = \frac{(+1)^k}{2}(L_k - L_{k+1})$$

which is a result of picking $c = 0$.

Examples of ESFR Scheme - Spectral Difference

By choosing $c = \frac{2k}{(2k+1)(k+1)(a_k k!)^2}$, the resulting flux correction functions are

$$g_L = \frac{(-1)^k}{2}(1 - x)L_k \ , \ g_R = \frac{(+1)^k}{2}(1 + x)L_k$$

Examples of ESFR Scheme - Hyuhn Type FR Scheme

If the value of c is set equal to $\frac{2(k+1)}{(2k+1)k(a_k k!)^2}$, the resulting flux correction functions are

$$g_L = \frac{(-1)^k}{2}\left[L_k - \left(\frac{(k+1)L_{k-1} + kL_{k+1}}{2k+1}\right)\right] \ , \ g_R = \frac{(+1)^k}{2}\left[L_k + \left(\frac{(k+1)L_{k-1} + kL_{k+1}}{2k+1}\right)\right]$$

PROOF OF STABILITY OF VCJH SCHEMES FOR DIFFUSION EQUATION

Stability of VCJH Schemes for Diffusion Equation

- Consider the heat equation

$$\frac{\partial u}{\partial t} - \frac{\partial^2 u}{\partial x^2} = 0 \tag{1}$$

which can be written as

$$\frac{\partial u}{\partial t} + \frac{\partial f}{\partial x} = 0 \tag{2}$$

where $f = f(u, \frac{\partial u}{\partial x}) = -\frac{\partial u}{\partial x}$.

Stability of VCJH Schemes for Diffusion Equation

- Using the flux reconstruction approach, the approximation solution u^δ is updated using

$$\frac{\partial u^\delta}{\partial t} = -\frac{\partial f^{\delta D}}{\partial x} - \frac{\partial g_L}{\partial x}(f_L^{\delta I} - f_L^{\delta D}) - \frac{\partial g_R}{\partial x}(f_R^{\delta I} - f_R^{\delta D}) \tag{3}$$

where $f^{\delta D}$ is a polynomial of order p which interpolates the values of the flux at the solution points, i.e.

$$f^{\delta D}(x) = \sum_i f_i^{\delta D} l_i(x) \tag{4}$$

g_L and g_R are corrections functions associated with the left and right interface, respectively and $f_L^{\delta I}$ and $f_R^{\delta I}$ are common flux values at the interfaces.

Stability of VCJH Schemes for Diffusion Equation

- The values of the discontinuous flux at the solution points ($f_i^{\delta D}$) are computed based on an approximation to the gradient of the solution, q^δ which is constructed as follows

$$q^\delta = \frac{\partial u^\delta}{\partial x} + \frac{\partial h_L}{\partial x}(u_L^{\delta I} - u_L^\delta) + \frac{\partial h_R}{\partial x}(u_R^{\delta I} - u_R^\delta) \tag{5}$$

where h_L and h_R are correction functions, $u_L^{\delta I}$ and $u_R^{\delta I}$ are common values of the solution at the interfaces. Hence,

$$f_i^{\delta D} = f(u^\delta(x_i), q^\delta(x_i)) \tag{6}$$

Stability of VCJH Schemes for Diffusion Equation

- If the correction functions g_L, g_R, h_L and h_R are the VCJH correction functions, which satisfy

$$-\int_{-1}^{1} g_L \frac{\partial u^\delta}{\partial x} dx + c \int_{-1}^{1} \frac{\partial^{p+1} g_L}{\partial x^{p+1}} \frac{\partial^p u^\delta}{\partial x^p} dx = 0 \tag{7}$$

$$-\int_{-1}^{1} g_R \frac{\partial u^\delta}{\partial x} dx + c \int_{-1}^{1} \frac{\partial^{p+1} g_R}{\partial x^{p+1}} \frac{\partial^p u^\delta}{\partial x^p} dx = 0 \tag{8}$$

$$-\int_{-1}^{1} h_L \frac{\partial q^\delta}{\partial x} dx + \kappa \int_{-1}^{1} \frac{\partial^{p+1} h_L}{\partial x^{p+1}} \frac{\partial^p q^\delta}{\partial x^p} dx = 0 \tag{9}$$

$$-\int_{-1}^{1} h_R \frac{\partial q^\delta}{\partial x} dx + \kappa \int_{-1}^{1} \frac{\partial^{p+1} h_R}{\partial x^{p+1}} \frac{\partial^p q^\delta}{\partial x^p} dx = 0 \tag{10}$$

where c and κ are arbitrary constants, and ...

Stability of VCJH Schemes for Diffusion Equation

if the common interface values of $u^{\delta I}$ and $f^{\delta I}$ are chosen as

$$f^{\delta I} = \frac{(f^+ + f^-)}{2} + \frac{\gamma}{2}(f^+ - f^-) \tag{11}$$

and

$$u^{\delta I} = \frac{(u^+ + u^-)}{2} - \frac{\gamma}{2}(u^+ - u^-) \tag{12}$$

then one can show that, for the heat equation,

$$\frac{1}{2}\frac{\partial}{\partial t}||u^{\delta}||^2_{p,c} = -||q^{\delta}||^2_{p,\kappa} \tag{13}$$

where the norm $||\cdot||_{p,c}$ is defined as

$$||w||^2_p = \int_{-1}^{1}\left[w^2 + c\left(\frac{\partial^p w}{\partial x^p}\right)^2\right]dx \tag{14}$$

FR approach on Triangles

Recent research on triangles

- The stability of the NDG scheme on triangle is well estabilished
- Numerical experiments have indicated that the SD schemes for triangles in the form proposed by Liu, Wang and Vinokur is not stable.
- May has shown that introducing Raviart Thomas basis functions to represent the flux can yield stable schemes
- Z.J. Wang has suggested the LCP scheme as a generalization of FR to triangles
- Using the flux reconstruction formulation we have been able to derive energy stable schemes of all orders of accuracy for triangles corresponding to the VCJH schemes.

FR approach on Triangles

- As in 1D, $\hat{\mathbf{f}}^{\delta}$ is written as the sum of a discontinuous flux and correction flux

$$\hat{\mathbf{f}}^{\delta} = \hat{\mathbf{f}}^{\delta D} + \hat{\mathbf{f}}^{\delta C}$$

- Discontinuous flux $\hat{\mathbf{f}}^{\delta D}$ is approximated by:

$$\hat{\mathbf{f}}^{\delta} = \sum_{i=1}^{N_p} \hat{\mathbf{f}}_i^{\delta D} l_i$$

where

$$\hat{\mathbf{f}}_i^{\delta D} = \hat{\mathbf{f}}(\hat{u}_i^{\delta})$$

FR approach on Triangles

Correction flux $\hat{\mathbf{f}}^{\delta C}$ takes the form:

$$\hat{\mathbf{f}}^{\delta C} = \sum_{f=1}^{3} \sum_{j=1}^{p+1} \left[(\hat{\mathbf{f}} \cdot \mathbf{n})^{\delta I}_{f,j} - ((\hat{\mathbf{f}} \cdot \mathbf{n})^{\delta D}_{f,j} \right] \mathbf{h}_{f,j}$$

- $(\hat{\mathbf{f}} \cdot \mathbf{n})^{\delta D}_{f,j}$ is the normal discontinuous flux value at flux points f, j
- $(\hat{\mathbf{f}} \cdot \mathbf{n})^{\delta I}_{f,j}$ is a numerical flux (common for both cells sharing that flux point)
- $(\hat{\mathbf{f}} \cdot \mathbf{n})^{\delta I}_{f,j}$ computed from a Riemann solver (Roe or Rusanov for example)

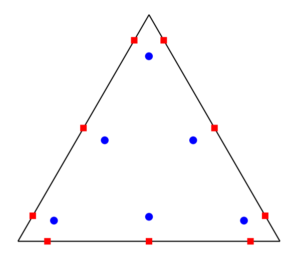

Flux points (squares)

FR approach on Triangles

In 2D, $\mathbf{h}_{f,j}$ is a vector correction function associated with flux point f, j. Correction functions $\mathbf{h}_{f,j}$ satisfy:

1. $\mathbf{h}_{f,j}$ is in Raviart-Thomas space of order p which implies
   - $\mathbf{h}_{f,j} \cdot \hat{\mathbf{n}}$ is polynomial of order p along each edge
   - $\nabla \cdot \mathbf{h}_{f,j}$ is polynomial of order p
2. $$\mathbf{h}_{f,j}(\mathbf{r}_{f_2,j_2}) \cdot \mathbf{n}_{f_2,j_2} = \begin{cases} 1 & \text{if } f = f_2 \text{ and } j = j_2 \\ 0 & \text{if } f \neq f_2 \text{ or } j \neq j_2 \end{cases}$$

Because of those properties, total flux $\hat{\mathbf{f}}^{\delta}$ is continuous everywhere along each edge

FR approach on Triangles

Example of a correction function $\mathbf{h}_{f,j}$ for $p = 2$:

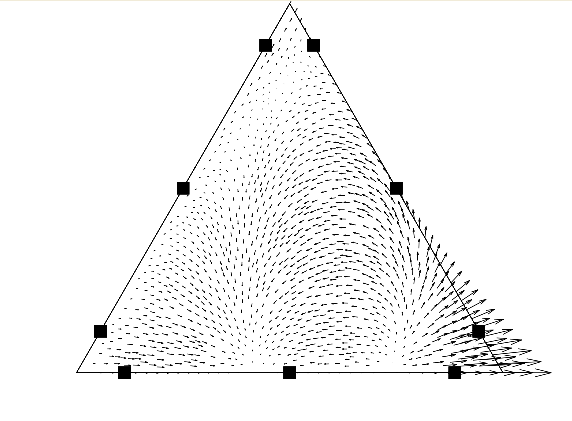

FR approach on Triangles

- Can recover collocation-based nodal DG scheme if each correction function $\mathbf{h}_{f,j}$ satisfies

$$\int_{\mathbf{\Omega}_S} \mathbf{h}_{f,j} \cdot \nabla_{rs} l_i \, d\mathbf{\Omega}_S = 0, \qquad \text{for } i = 1 \text{ to } N_p$$

- Using divergence theorem, can solve for $\phi_{f,j} = \nabla_{rs} \cdot \mathbf{h}_{f,j}$ directly from

$$\int_{\mathbf{\Omega}_S} \phi_{f,j} l_i d\mathbf{\Omega}_S = \int_{\mathbf{\Gamma}_S} \left(\mathbf{h}_{f,j} \cdot \hat{\mathbf{n}}\right) l_i d\mathbf{\Gamma}_S, \qquad \text{for } i = 1 \text{ to } N_p$$

VCJH Schemes on Triangles

Linear stability guaranteed if correction functions $\mathbf{h}_{f,j}$ satisfy

$$\kappa \sum_{m=1}^{p+1} \binom{p}{m-1} \left(D^{(m,p)} L_i\right) \left(D^{(m,p)}(\nabla \cdot \mathbf{h}_{f,j})\right) = \int_{\mathbf{\Omega}_S} \mathbf{h}_{f,j} \nabla L_i d\mathbf{\Omega}_S$$

for $1 \leq i \leq N_p$, where

- $$D^{(m,p)} = \frac{\partial^p}{\partial r^{(m-p+1)} \partial s^{(m-1)}}$$
- L_i are members of an orthonormal basis (Dubiner basis)
- $\binom{p}{m-1}$ are binomial coefficients
- κ is a scalar which must be greater than 0

VCJH Schemes on Triangles

- The form of each correction fields $\phi_{f,j}$ is obtained by solving system of equations on previous slide
- As in 1D, we have a family of linearly stable high-order methods on triangles, which are parameterized by a single scalar coefficient κ
- By setting $\kappa = 0$, recover a collocation-based nodal DG scheme
- Have yet to verify if other high-order methods can be recovered

VCJH Schemes on Triangles

Accuracy has been investigated for linear advection equation in 2D on unstructured triangular grid for $\kappa = 0$ and $\kappa = \kappa_+$

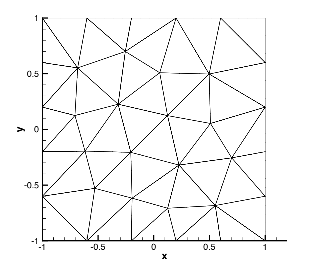

Measure of accuracy:

$$L_2 \text{ error } = \sqrt{\frac{\sum_{n=1}^{N} \sum_{i=1}^{N_p} \left(u_{i,n} - u_{i,n}^e\right)^2}{N \cdot N_p}}$$

VCJH Schemes on Triangles

Numerical Experiment on advection equation in 2D

p	Grid Size	$\kappa = 0$ L_2 error	Order	$\Delta t'_{max}$	$\kappa = \kappa_+$ L_2 error	Order	$\Delta t'_{max}$
2	$5 \times 5 \times 2$	3.922e-02	-	0.288	1.362e-01	-	0.568
	$10 \times 10 \times 2$	5.336e-03	2.82	0.272	2.131e-02	2.68	0.558
	$20 \times 20 \times 2$	7.350e-04	2.91	0.262	2.947e-03	2.85	0.554
	$40 \times 40 \times 2$	8.997e-05	3.03	0.254	3.720e-04	2.99	0.522
	$80 \times 80 \times 2$	1.107e-05	3.02	0.250	4.660e-05	3.00	0.504
3	$5 \times 5 \times 2$	5.690e-03	-	0.190	1.605e-02	-	0.346
	$10 \times 10 \times 2$	3.094e-04	3.87	0.178	1.211e-03	3.73	0.336
	$20 \times 20 \times 2$	2.456e-05	3.99	0.168	7.809e-05	3.95	0.324
	$40 \times 40 \times 2$	1.523e-06	4.01	0.160	4.910e-06	3.99	0.316
	$80 \times 80 \times 2$	9.519e-08	4.00	0.150	3.069e-07	4.00	0.308
4	$5 \times 5 \times 2$	6.801e-04	-	0.136	1.842e-03	-	0.232
	$10 \times 10 \times 2$	2.066e-05	5.04	0.130	5.424e-05	5.09	0.224
	$20 \times 20 \times 2$	6.982e-07	4.89	0.124	1.803e-06	4.91	0.216
	$40 \times 40 \times 2$	2.128e-08	5.04	0.120	5.449e-08	5.05	0.212

IMPLEMENTATION

Overview of Flow Solver Development

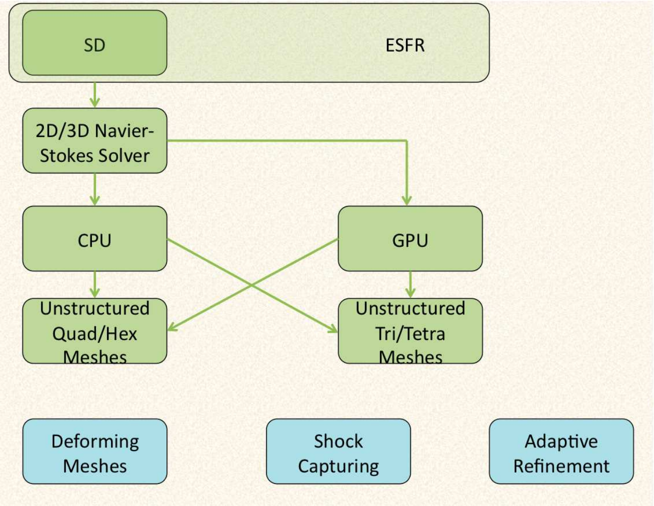

Current Status of Flow Solvers Based on GPUs

CPU: Xeon X5670
- 6 cores
- 2.93 Ghz
- 32 GB/s bandwidth

GPU: Tesla C2050
- 14 SM's x 1536 threads
- 1.15 Ghz, 448 cores
- 144 GB/s bandwidth
- Peak performance (double): 515 Gflops

Desktop cluster of 3 Tesla C2050 GPUs
- Speed equivalent to 240 Intel Xeon 5670 2.93GHz CPU cores

Current Status of Flow Solvers Based on GPUs

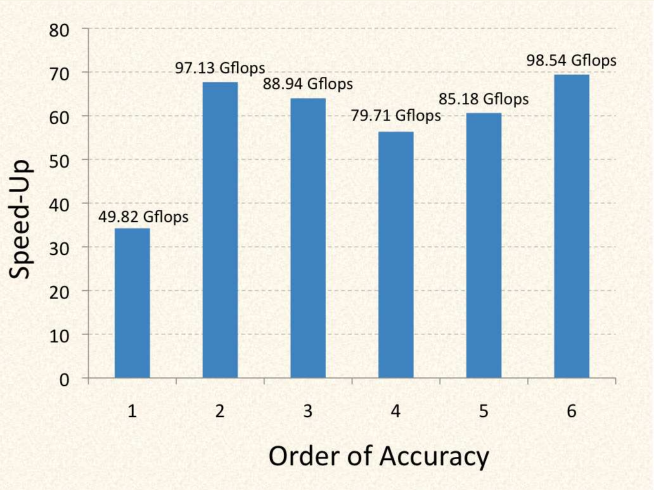

Current Status of Flow Solvers Based on GPUs

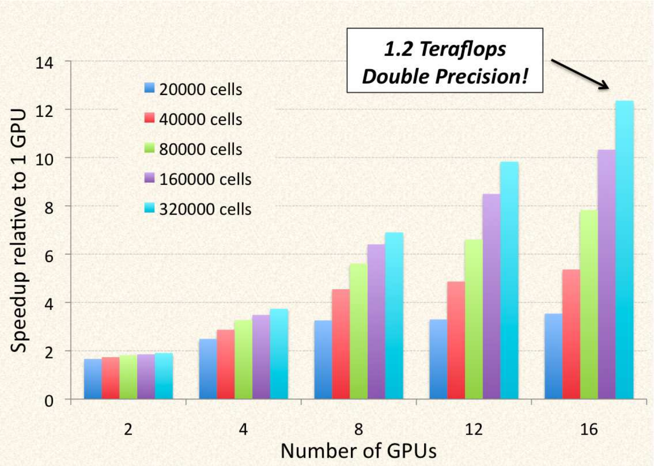

Applications

Airfoils and Wings

SD7003 Airfoil at Re=40,000 at 4^o angle of attacks

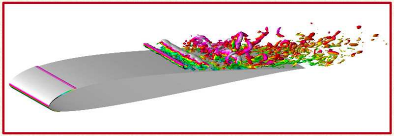

Eppler61 Airfoil at Re=46,000 at 6^o, 8^o, 10^o, 12^o, and 14^o angle of attacks

Airfoils and Wings

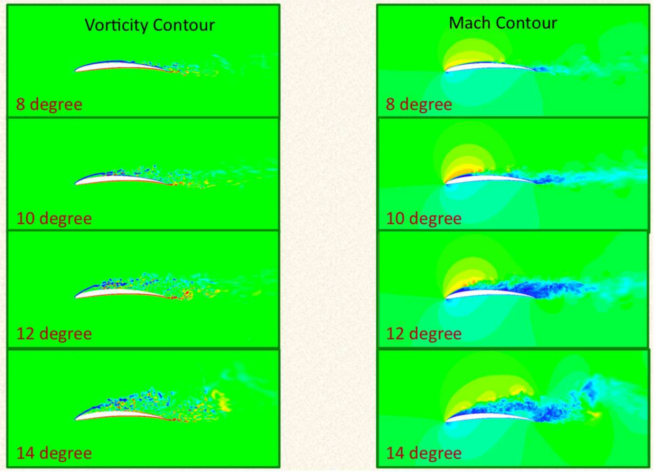

Airfoils and Wings

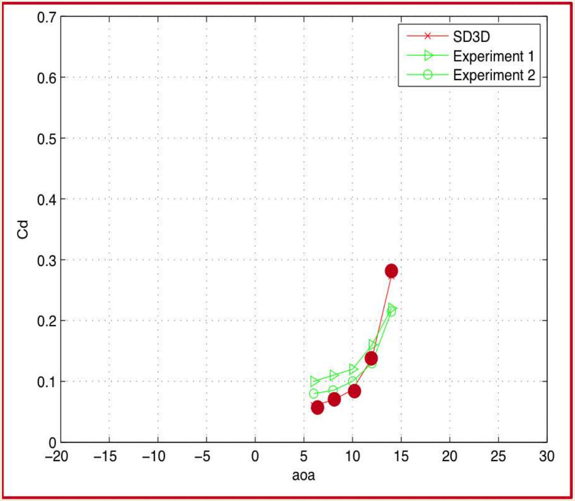

Airfoils and Wings

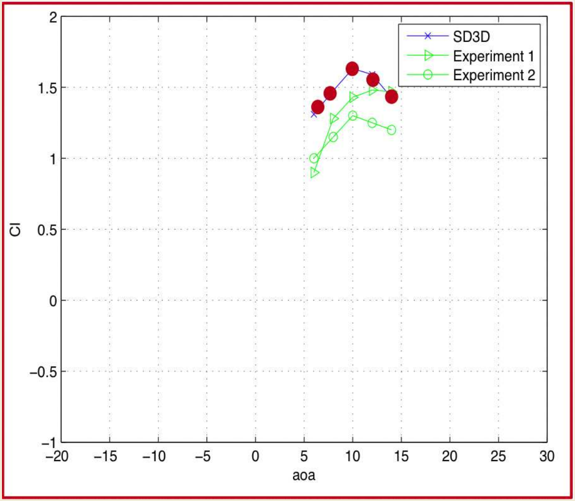

Airfoils and Wings

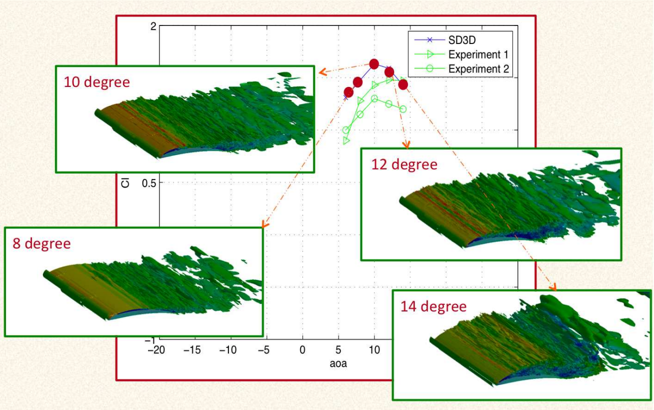

Airfoils and Wings

Movie of Transitional Flow over a Plunging SD7003

(Video)

Airfoils and Wings

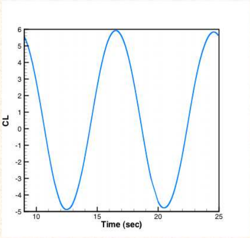

(a) CL Time History with SD3D

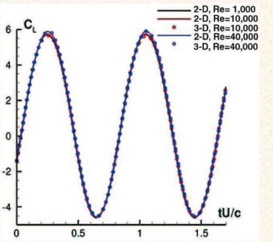

(b) CL Time History from Visbal's study[14]

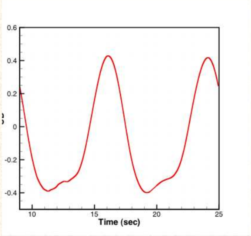

(a) CD Time History with SD3D

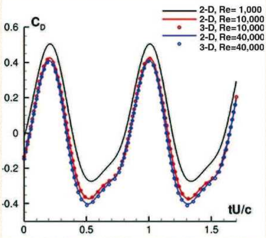

(b) CD Time History from Visbal's study[14]

Sphere and Torus

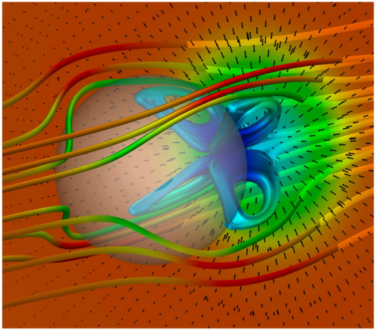

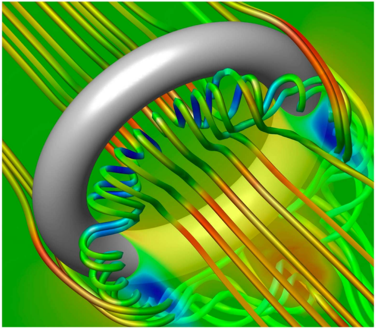

Spinning Sphere

Movie of a Spinning Sphere

(Video)

Complete Configurations - Flapping Wing Vehicle

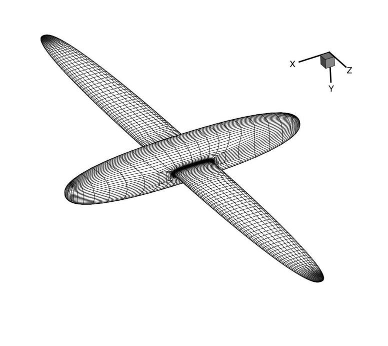

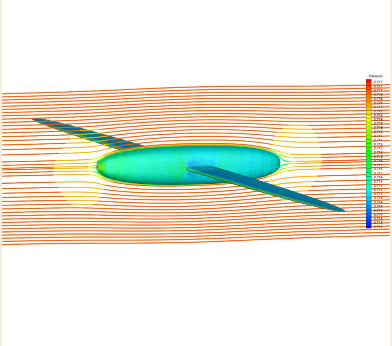

Flapping Wing Vehicle

Movie of a Flapping Wing Vehicle

(Video)

Complete Configurations - Predator

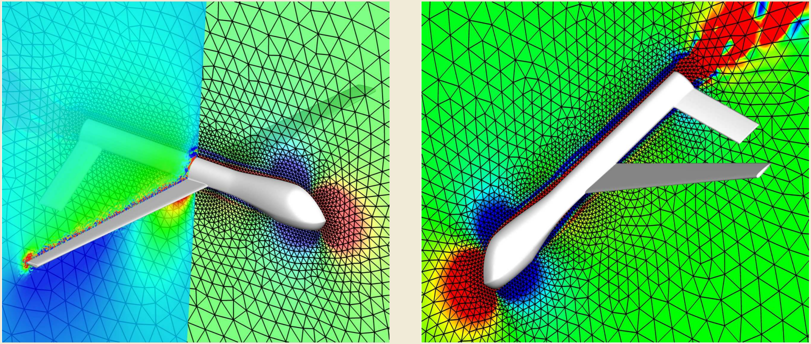

Closing Remarks

Conclusions

- CFD has been on a plateau of Raynolds Averaged Navier-Stokes (RANS) simulaitons for the past 15 years. These are not adequate for vortex dominated and transitional flows such as rotorcraft, flapping wing MAV, or high-lift systems
- Rapid advances in computer hardware will enable a transition to large eddy simulation (LES) for industrial applications with complex geometry within the foreseeable future.
- High-order methods for unstructured meshes provide an essential building block for LES which can capture the bulk of the turbulent energy.
- Advances in subgrid modeling for wall bounded flows will also be needed. We are performing preliminary tests of SD and FR simulations with a wall adopted similarity model.
- These advances can also provide a basis for aero-accoustic simulations of airframe noise emanating from landing gear or high-lift systems.

Questions and Answers